

Detection of the white dwarf and the secondary star in the new SU UMa dwarf nova HS 2219+1824 *

P. Rodríguez-Gil¹, B. T. Gänsicke¹, H.-J. Hagen², T. R. Marsh¹, E. T. Harlaftis³, S. Kitsionas⁴, and D. Engels²

¹ Department of Physics, University of Warwick, Coventry CV4 7AL, UK

² Hamburger Sternwarte, Universität Hamburg, Gojenbergsweg 112, 21029 Hamburg, Germany

³ Institute of Space Applications and Remote Sensing, National Observatory of Athens, P.O. Box 20048, Athens 11810, Greece

⁴ Institute of Astronomy and Astrophysics, National Observatory of Athens, P.O. Box 20048, Athens 11810, Greece

Received 2004; accepted 2004

Abstract. We report the discovery of a new, non-eclipsing SU UMa-type dwarf nova, HS 2219+1824. Photometry obtained in quiescence ($V \approx 17.5$) reveals a double-humped light curve from which we derive an orbital period of $\simeq 86.2$ min. Additional photometry obtained during a superoutburst reaching $V \simeq 12.0$ clearly shows superhumps with a period of $\simeq 89.05$ min. The optical spectrum contains double-peaked Balmer and He I emission lines from the accretion disc as well as broad absorption troughs of H β , H γ , and H δ from the white dwarf primary star. Modelling of the optical spectrum implies a white dwarf temperature of $13\,000\text{ K} \lesssim T_{\text{eff}} \lesssim 17\,000\text{ K}$, a distance of $180\text{ pc} \lesssim d \lesssim 230\text{ pc}$, and suggests that the spectral type of the donor star is later than M5. Phase-resolved spectroscopy obtained during quiescence reveals a narrow H α emission line component which has a radial velocity amplitude and phase consistent with an origin on the secondary star, possibly on the irradiated hemisphere facing the white dwarf. This constitutes the first detection of line emission from the secondary star in a quiescent SU UMa star.

Key words. accretion, accretion discs – binaries: close – stars: individual: HS 2219+1824 – novae, cataclysmic variables

1. Introduction

We are currently pursuing a large-scale survey for cataclysmic variables (CVs), selecting candidates by the detection of Balmer emission lines in the spectroscopic data from the Hamburg Quasar Survey (Gänsicke

et al. 2002). So far, this survey has proved to be very efficient in identifying CVs that are relatively bright at optical wavelengths but are characterised by either low-amplitude variability, or by long outburst recurrence times, or by low X-ray luminosities. Examples of systems discovered or independently identified in our program include the deeply eclipsing, long-period dwarf nova GY Cnc (= HS 0907+1902, Gänsicke et al. 2000), the rarely outbursting SU UMa-type dwarf nova KV Dra (= HS 1449+6415, Nogami et al. 2000), the two intermediate polars 1RXS J062518.2+733433 (= HS 0618+7336, Araujo-Betancor et al. 2003) and DW Cnc (= HS 0756+1624, Rodríguez-Gil et al. 2004a), the SW Sex stars KUV 03580+0614 (= HS 0357+0614, Szkody et al. 2001) and HS 0728+6738 (Rodríguez-Gil et al. 2004b), and the old pre-CV HS 2237+8154 (Gänsicke et al. 2004). Whereas all these systems belong to species that are currently rare in the overall population of known CVs, their intrinsic number may be comparable to, if not larger than, that of the “classic” CVs, which are either

Send offprint requests to: P. Rodríguez-Gil,
e-mail: Pablo.Rodriguez-Gil@warwick.ac.uk

* Based in part on observations obtained at the German-Spanish Astronomical Center, Calar Alto, operated by the Max-Planck-Institut für Astronomie, Heidelberg, jointly with the Spanish National Commission for Astronomy; on observations made with the IAC80 and OGS telescopes, operated on the island of Tenerife by the Instituto de Astrofísica de Canarias (IAC) and the European Space Agency (ESA), respectively, in the Spanish Observatorio del Teide of the IAC; on observations made at the 1.2 m telescope, located at Kryoneri Korinthias, and owned by the National Observatory of Athens, Greece; and on observations made with the William Herschel Telescope, which is operated on the island of La Palma by the Isaac Newton Group in the Spanish Observatorio del Roque de los Muchachos of the IAC.

Table 1. Log of observations.

Date	UT	Filter/ Grating	Mag.	Exp. (s)	Frames
2.2 m Calar Alto					
2000 Sep 20	22:26 - 22:40	B – 200 R – 200	$V \simeq 17.3$	600	1/1
1.2 m Kryoneri Observatory					
2002 Sep 17	00:36 - 03:16	R	$\simeq 17.6$	90	97
2002 Sep 17	22:40 - 23:11	R	$\simeq 17.5$	60	25
2002 Sep 18	19:04 - 23:41	R	$\simeq 17.6$	60	210
1 m OGS					
2003 Jul 08	03:27 - 05:24	Clear	$\simeq 15.7$	15	390
2003 Jul 10	01:21 - 03:47	Clear	$\simeq 12.2$	15	515
2003 Jul 11	02:47 - 04:06	Clear	$\simeq 12.2$	12	37
2003 Jul 14	01:21 - 03:59	Clear	$\simeq 12.5$	12	548
2003 Jul 16	02:20 - 05:31	Clear	$\simeq 12.8$	12	617
0.82 m IAC80					
2003 Sep 25	00:19 - 03:14	Clear	$\simeq 17.4$	70	74
2003 Sep 26	00:32 - 03:14	Clear	$\simeq 17.5$	70	119
2003 Sep 27	23:31 - 03:10	Clear	$\simeq 17.5$	70	160
2003 Sep 28	20:01 - 23:35	Clear	$\simeq 17.5$	70	147
4.2 m WHT					
2003 Oct 19	19:35 - 22:58	R600B R316R		400	28

frequently in outburst, or X-ray bright, or display obvious photometric variability.

Here we report the discovery of a new short-period, SU UMa-type dwarf nova with long recurrence time outbursts, HS 2219+1824. This system belongs to the relatively small group of dwarf novae whose optical spectra clearly reveal the photospheric emission of their white dwarf primary stars. More exceptional is, however, the fact that we detect in the quiescent spectrum of HS 2219+1824 a narrow $H\alpha$ emission line component which we believe to originate on the secondary star.

By inspection of the available sky surveys we discovered that the USNO–A2.0 catalogue shows HS 2219+1824 in outburst with $B = 12.9$ and $R = 13.6$. Both DSS 1 and DSS 2 show the system in quiescence. ASAS-3 (Pojmański 2001) monitored HS 2219+1824 on 72 occasions between April 2003 and August 2004, and detected the July 2003 August superoutburst (also observed by us) as well as a second superoutburst reaching $V \simeq 11.8$ on June 24 2004. Even though sparse, the data collected so far shows that HS 2219+1824 does not belong to the class of WZ Sge dwarf novae with recurrence times of tens of years. So far, no normal outburst of HS 2219+1824 has been recorded.

We describe our observational data in Sect. 2, the analysis of the photometry and spectroscopy in Sect. 3 and Sect. 4, respectively, and discuss on the system parameters of HS 2219+1824 in Sect. 5.

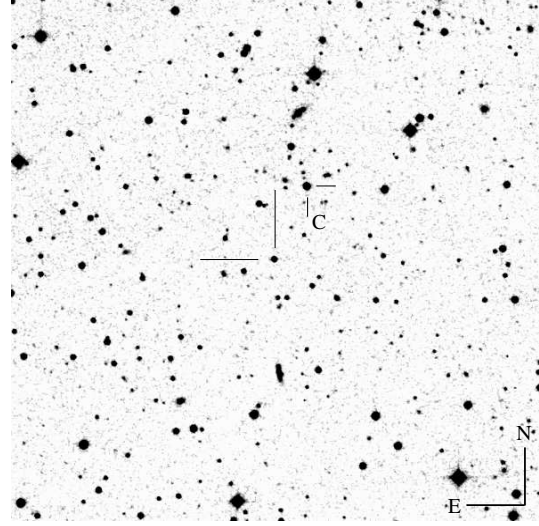


Fig. 1. $10' \times 10'$ finding chart of HS 2219+1824 obtained from the Digitized Sky Survey 2. The coordinates of the CV are $\alpha(2000) = 22^h 21^m 44.8^s$, $\delta(2000) = +18^\circ 40' 08.3''$. The star ‘C’ has been used as comparison for all the differential photometric data.

2. Observations and data reduction

2.1. Spectroscopy: Calar Alto

A pair of blue/red identification spectra of HS 2219+1824 was obtained at the 2.2 m Calar Alto telescope with the CAFOS spectrograph (Table 1). We used the B-200 and R-200 gratings in conjunction with a $2''$ slit, providing a spectral resolution of $\simeq 10 \text{ \AA}$ (FWHM). A standard reduction of these data was carried out using the CAFOS MIDAS quicklook package. The detection of strong Balmer emission lines confirmed the CV nature of HS 2219+1824 and triggered the additional follow-up observations described below. The CAFOS acquisition image obtained just before the B-200/R-200 spectroscopy showed HS 2219+1824 at $V \simeq 17.3$.

2.2. Photometry: Kryoneri

Differential R -band photometry of HS 2219+1824 was obtained in 2002 September/October using the 1.2 m Kryoneri telescope equipped with a SI-502 $516 \times 516 \text{ pixel}^2$ CCD camera (Table 1). Aperture photometry was carried out on all images using the MIDAS & SEXTRACTOR (Bertin & Arnouts 1996) pipeline described by Gänsicke et al. (2004). The differential magnitudes of HS 2219+1824 were derived relative to the comparison star USNO–A2.0 1050–20233792, labelled ‘C’ in Fig. 1. The differential measurements were converted into R -band magnitudes using the USNO–A2.0 magnitude of the comparison star, $R_{\text{comp}} = 15.4$. The main source of uncertainty in this conversion is the uncertainty in the USNO magnitudes, which is typically $\simeq 0.2 \text{ mag}$.

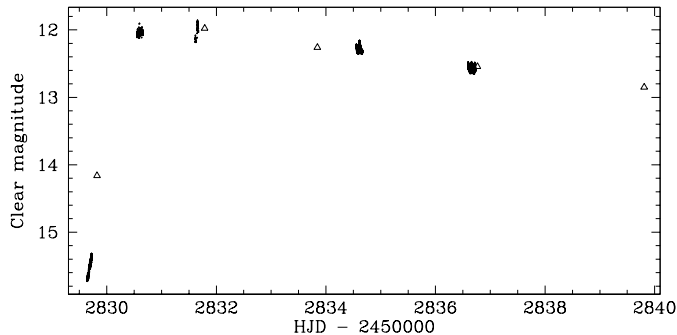


Fig. 2. Superoutburst of HS 2219+1824 recorded at the OGS telescope. Superhumps set in ~ 1 d after the outburst maximum. The filterless magnitudes are approximatively equivalent to V-band data. Shown as open triangles are the V magnitudes of HS 2219+1824 from the ASAS-3 archive.

2.3. Photometry: OGS

The 1 m Optical Ground Station (OGS) telescope at the Observatorio del Teide on Tenerife was also used to perform time-resolved photometry of HS 2219+1824. The data were obtained between 2003 July 7 and 15 (Table 1) using the Thomson 1024×1024 pixel² CCD camera and no filter. Exposure times of 12 and 15 seconds (depending on sky transparency) were adopted and 2×2 binning and windowing were applied to improve the time resolution. The raw images were de-biased and flat-field compensated, and the instrumental magnitudes were obtained with the Point Spread Function (PSF)-fitting packages within IRAF¹. Differential light curves were then computed relative to the same comparison star used for the Kryoneri data.

The second night of observation at the OGS telescope offered us an unusually bright HS 2219+1824. Comparison with the brightness measured on the previous night showed that the object had brightened by nearly four magnitudes, indicating that an outburst was in progress. The subsequent detection of superhumps (see Fig. 2 and Sect. 3.2) confirmed that the brightening was actually an SU UMa-like superoutburst.

The July 2003 superoutburst was also recorded by ASAS-3 (Pojmański 2001), and the V magnitudes from the ASAS-3 archive are plotted along with the OGS data in Fig. 2.

2.4. Photometry: IAC80

Additional filterless photometry of HS 2219+1824 was obtained in October 2003 with the 0.82 m IAC80 telescope on Tenerife using the Thomson 1024×1024 pixel² CCD camera and an exposure time of 70 s (Table 1). Only a small part of the CCD was read out (in binning 2×2 mode) in

¹ IRAF is distributed by the National Optical Astronomy Observatories, which is operated by the Association of Universities for Research in Astronomy, Inc., under contract with the National Science Foundation.

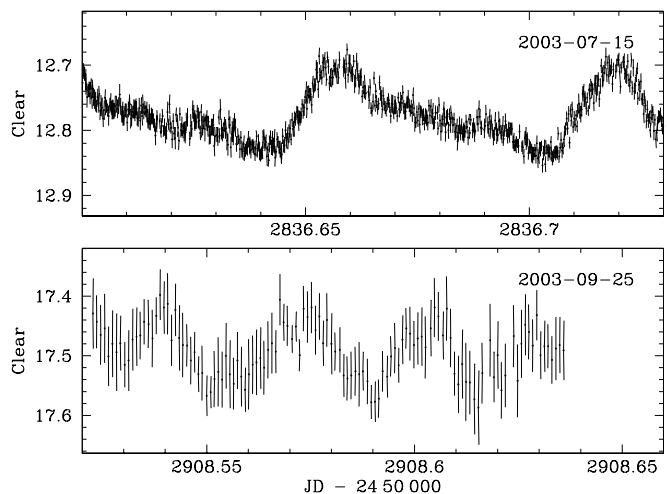


Fig. 3. Sample light curves of HS 2219+1824 obtained during the superoutburst (top panel) and in quiescence (bottom panel).

order to improve the time resolution. The data were reduced in the same fashion as described above for the OGS (Sect. 2.3). Differential magnitudes of HS 2219+1824 were derived using the comparison star 'C' (Fig. 1). The average magnitude of ~ 17.5 mag indicates that HS 2219+1824 was in quiescence during the IAC80 observations.

2.5. Spectroscopy: William Herschel Telescope

Time-resolved spectroscopy of HS 2219+1824 in quiescence was performed on the night of 2003 October 19 with the 4.2 m William Herschel Telescope (WHT) on La Palma and the ISIS spectrograph. The blue arm was equipped with the R600B grating and the 2048×4100 pixel² EEV12 CCD camera, while the R316R grating and the 2047×4611 pixel² Marconi CCD were in place on the red arm. A $1''$ slit gave a spectral resolution of 1.8 and 3.2 Å (FWHM), respectively, covering the wavelength ranges $\lambda\lambda 4000 - 5000$ and $\lambda\lambda 6100 - 9240$. The small pixel size of both detectors produces oversampling of the best possible resolution, so we applied a 1×2 binning (dispersion direction) on both chips. This increased the signal in each wavelength bin without losing spectral resolution.

A total of 28 blue and red spectra were obtained with an exposure time of 400 seconds (see Table 1). Spectra of the combined light of Cu-Ar and Cu-Ne arc lamps were taken regularly in order to achieve an optimal wavelength calibration. The raw images were de-biased, flat-fielded and sky-subtracted in the standard way. The target spectra were then optimally extracted (Horne 1986). These reduction processes were carried out within IRAF. A third-order polynomial was fitted to the arc wavelength-pixel function, the *rms* being always less than one tenth of the spectral dispersion on each arm.

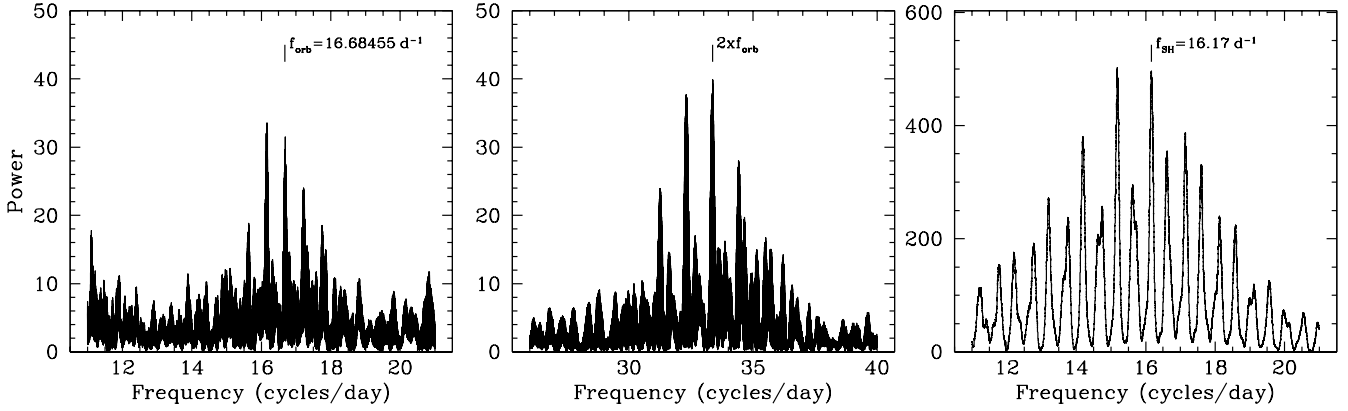


Fig. 4. Left and middle panels: AOV periodograms of the entire quiescent data (Kryoneri & IAC80). Right panel: AOV periodogram of the superoutburst data (OGS, 2003 July 11, 14 & 16).

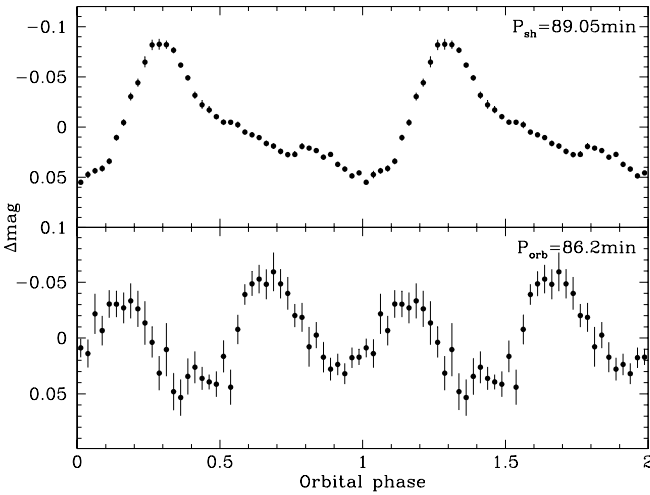


Fig. 5. Top panel: Superoutburst photometry obtained on 2003 July 11, 14 & 16 folded over the superhump period of $P_{sh} = 89.05$ min and averaged into 40 phase bins. Bottom panel: Quiescent photometry (Kryoneri 2002 and IAC80 2003) folded over the orbital period of 86.2 min and averaged into 40 phase bins. In both cases, the mean magnitude of each individual night was subtracted before folding and binning. The orbital cycle has been duplicated for continuity.

3. Analysis: Photometry

3.1. Quiescence

During quiescence, the light curve of HS 2219+1824 displays a hump-like structure with an amplitude of ~ 0.05 mag and a period of ~ 40 min (bottom panel of Fig. 3). The analysis-of-variance periodograms (AOV, Schwarzenberg-Czerny 1989) computed from the Kryoneri and IAC80 quiescent data (Fig. 4) confirm this visual estimate, showing strong signals at $\simeq 43.1$ min ($\simeq 33.4$ d $^{-1}$) and $\simeq 44.6$ min ($\simeq 32.3$ d $^{-1}$). Significant power is also found at twice these periods. By analogy to a number of short-period CVs which show quiescent orbital light curves dominated by a double-humped structure

(WX Cet: Mennickent 1994; WZ Sge: Patterson 1998; RZ Leo, BC UMa, MM Hya, HV Vir: Patterson et al. 2003; HS 2331+3905: Araujo-Betancor et al. 2004), we identify the 43.1/44.6 min photometric periodicity with orbital variability, and hence $P_{orb} \simeq 86.2$ min or $P_{orb} \simeq 89.2$ min.

3.2. The superoutburst

Our July 2003 observations of HS 2219+1824 at the OGS caught the system on the rise to outburst. The duration of the event and the onset of superhumps clearly identify it as an SU UMa-type superoutburst. We have computed an AOV periodogram from the OGS data obtained on July 11, 14, and 16 (Fig. 4). The strongest signals are detected at $\simeq 15.17$ d $^{-1}$ ($\simeq 94.92$ min) and $\simeq 16.17$ d $^{-1}$ ($\simeq 89.05$ min). Both signals significantly differ from the two possible orbital periods determined from the quiescent photometry. The longer period ($> P_{orb}$) and the shape of the outburst light curve are characteristic of a superhump wave, triggered by the precession of an eccentric accretion disc. The fractional period excess $\epsilon = (P_{sh} - P_{orb})/P_{orb}$ is $\epsilon = 3.3\%$ for ($P_{orb} = 86.2$ min, $P_{sh} = 89.05$ min), and $\epsilon = 6.4\%$ for ($P_{orb} = 89.2$ min, $P_{sh} = 94.92$ min). No dwarf nova with $\epsilon > 5\%$ is known below the period gap (Patterson et al. 2003), which strongly suggests that $P_{orb} = 86.2$ min and $P_{sh} = 89.05$ min are indeed the orbital and superhump periods of HS 2219+1824. In Fig. 5 we show the superoutburst and quiescent light curves folded on 89.05 and 86.2 min, respectively.

4. Analysis: Spectroscopy

4.1. The optical spectrum of HS 2219+1824

The identification spectrum of HS 2219+1824 (Fig. 6) contains emission lines of neutral hydrogen and helium. The Balmer lines show a relatively strong decrement and H β to H γ are embedded in very broad absorption troughs. Similar broad Balmer absorption lines have been detected in a number of other short period dwarf novae, e.g.

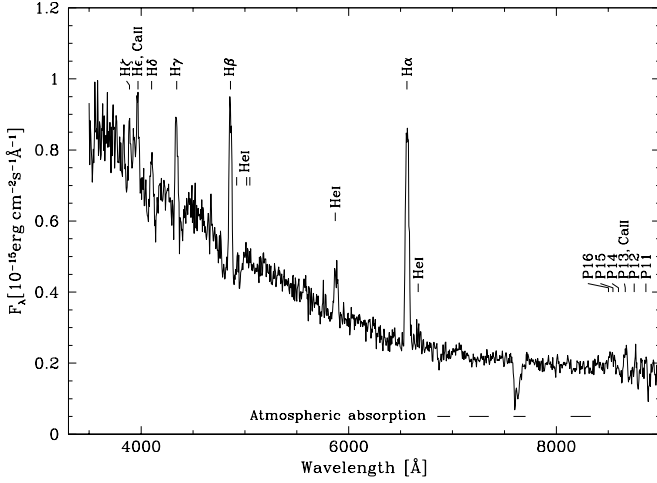


Fig. 6. Discovery spectrum of HS 2219+1824, obtained with the 2.2 m Telescope at Calar Alto.

WZ Sge (Greenstein 1957; Gilliland et al. 1986), GW Lib (Duerbeck & Seitter 1987), BC UMa (Mukai et al. 1990), or BW Scl (Abbott et al. 1997). In all these systems the hypothetical identification of the observed Balmer absorption as the photospheric spectrum of the white dwarf has been confirmed by the unambiguous detection of the white dwarf at ultraviolet wavelengths (Sion et al. 1990; Szkody et al. 2002; Gänsicke et al. 2004). The continuum displays a rather blue slope shortwards of H α , and a nearly flat slope at the red end of our spectrum. No strong TiO absorption lines, typical of mid-to-late M dwarfs are detected in the red part of the spectrum.

The emission lines are clearly double-peaked in the higher resolution WHT spectra (Fig. 7), a clear indication of the presence of an accretion disc in the system. Fig. 7 illustrates the evolution of the H α profile throughout our 2003 October 19 WHT/ISIS observations. The relative strength of the two peaks clearly changes with time, possibly indicating the presence of an emission S-wave moving inside the double peaks. Remarkably, many of the profiles seem to have three peaks, revealing the presence of another emission component in the lines (see right panel of Fig. 7).

4.2. A model for the optical continuum

Inspired by the similarity between the optical spectrum of HS 2219+1824 and those of e.g. WZ Sge, GW Lib, BC UMa or BW Scl (Sect. 4.1), which all reveal the spectra of their white dwarf primaries, we have modelled the identification spectrum of HS 2219+1824 with a simple three-component model accounting for the emission of the white dwarf, the accretion disc, and the secondary star. For the white dwarf, we use the model spectra of Gänsicke et al. (1995), and assume a surface gravity of $\log g = 8.0$ ($\simeq 0.6 M_{\odot}$). The radius of the white dwarf is determined from the Hamada & Salpeter (1961) mass-radius relation, $R_1 = 8.7 \times 10^8$ cm. Free parameters in the model are the

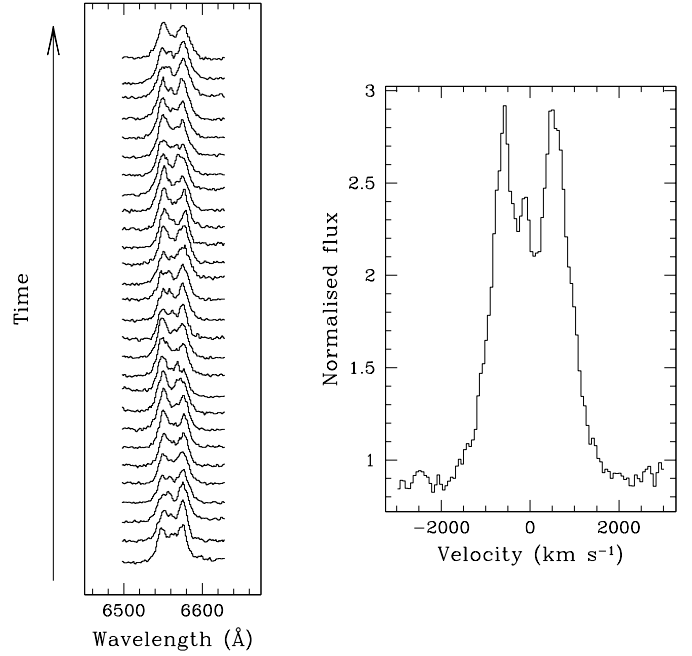


Fig. 7. *Left panel:* evolution of the H α profile during the WHT/ISIS observations. The time co-ordinate runs from UT 19:35 to UT 22:58 (see Table 1). *Right panel:* Selected H α profile displaying three peaks.

white dwarf effective temperature, T_{eff} , and the distance to HS 2219+1824. For the accretion disc, we use the isothermal/isobaric hydrogen slab model described by Gänsicke et al. (1997, 1999). Free parameters are the temperature of the slab T_{disc} , the column density along the line of sight Σ , and a flux scaling factor Ω . For the secondary star, we use the observed spectra of late-type main sequence stars from Beuermann et al. (1998) as templates. We assume an equivalent Roche-lobe radius of the secondary star of $R_{L2} = 9.5 \times 10^9$ cm, which corresponds to a mass ratio of $M_2/M_1 = 0.14$ at the orbital period of HS 2219+1824 (see the discussion in Sect. 5). Free parameters for the secondary star component are the spectral type Sp(2) and the distance to the system.

We started modelling of the observed optical spectrum of HS 2219+1824 by matching the width and depth of the H β to H δ absorption profiles with a synthetic white dwarf spectrum, and find $13\,000\text{ K} \lesssim T_{\text{eff}} \lesssim 17\,000\text{ K}$ and $180\text{ pc} \lesssim d \lesssim 230\text{ pc}$ – with the white dwarf contributing $\simeq 65\%$ at 5500 Å . In a second step, we add the emission of the isobaric slab, scaling it to the observed H α flux. The main parameter determining the Balmer decrement is T_{disc} , the optical depth ratio between the emission lines and the continuum primarily depends on Σ . An adequate match is found for $T_{\text{disc}} \simeq 6000\text{ K}$ and $\Sigma \simeq 5.7 \times 10^{-2}\text{ g cm}^{-2}$. The “disc” temperature is the canonical temperature expected for low mass transfer discs (Williams 1980). For a distance of $d \simeq 200\text{ pc}$, the radius of the “disc” implied by the flux scaling factor is $R_{\text{disc}} \simeq 2.3 \times 10^{10}$ cm, well within the Roche-lobe radius of

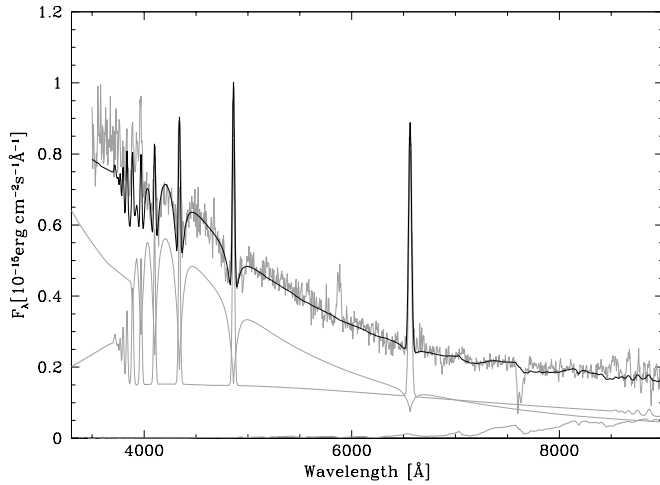


Fig. 8. Three-component model of the optical spectrum of HS 2219+1824. The observed spectrum is the topmost grey line. The grey lines below are a white dwarf model spectrum for $T_{\text{eff}} = 16000$ K, $\log g = 8.0$, and $d = 215$ pc (broad absorption lines), the emission from an isothermal/isobaric slab with $T_{\text{disc}} = 6000$ K and $\Sigma = 5.7 \times 10^{-2} \text{ g cm}^{-2}$, scaled to the observed H α flux (emission lines). The secondary star is represented by a M6 template, assuming $R_{L2} = 9.5 \times 10^9$ cm and $d = 215$ pc. The sum of the three components is plotted as black line.

the primary. This radius should, however, only be considered as a rough estimate, as it is based on the assumption of our very simplistic model for the disc emission. Finally, we add the spectral contribution of the secondary star. The observed flux at the red end of the optical spectrum constrains Sp(2) to be later than M5 for a distance of $d \simeq 200$ pc. A model for $T_{\text{eff}} = 16000$ K, Sp(2)=M6.0, $d = 215$ pc and the disc parameters as above is shown in Fig. 8.

4.3. Radial velocity curve analysis

The light curves obtained during quiescence revealed a double-humped variation at 86.2 min (see Sect. 3.1). In order to confirm that this value represents the actual orbital period of HS 2219+1824 we have analysed the radial velocity variations of the H α emission line, since this line is the least affected by the broad absorption. Prior to measuring the velocities the individual spectra were normalised using a low-order spline fit to the continuum. The emission lines and the broad absorptions were masked off the fitting procedure. We then resampled all the spectra on to a uniform velocity scale centred on the H α rest wavelength. We computed the radial velocity curves of H α using the technique of Schneider & Young (1980) for a Gaussian FWHM of 300 km s^{-1} and different values of the Gaussian separation ($a = 1200 - 2600 \text{ km s}^{-1}$ in steps of 100 km s^{-1}), following the technique of “diagnostic diagrams” (Shafter 1983; Shafter et al. 1995). A sine function was fitted to each curve to establish the K_1 velocity, and we find the

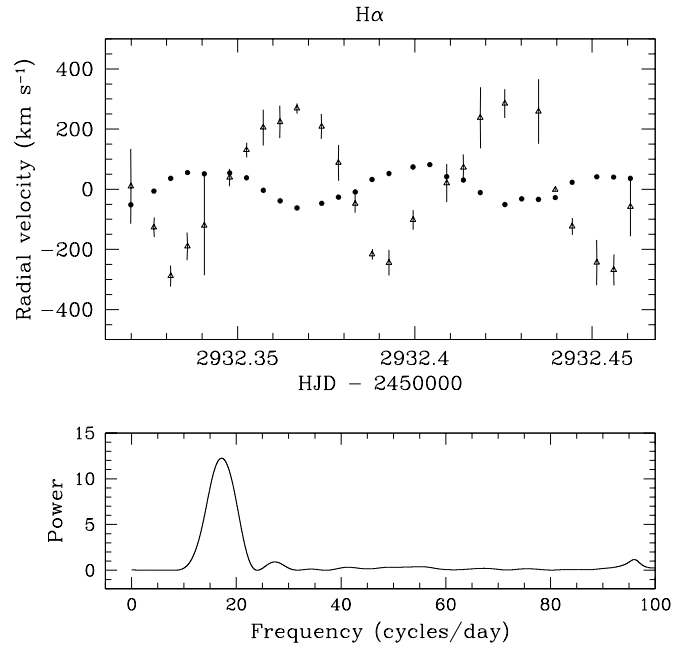


Fig. 9. *Top:* H α radial velocity curves of HS 2219+1824 in quiescence computed from the line wings (*filled circles*) and the narrow component (*open triangles*). *Bottom:* Scargle periodogram of the H α wing velocities.

maximum useful separation to be $a \simeq 2300 - 2400 \text{ km s}^{-1}$, where $K_1 \simeq 50 \text{ km s}^{-1}$. The H α radial velocity curve obtained is shown in the top panel of Fig. 9 (plotted as filled circles). A Scargle periodogram (Scargle 1982) of the velocities produced a broad peak centred at a period of ~ 85 min. A sine fit to the curve yielded a period of 84.9 ± 0.9 min, which is consistent with the more accurate photometric determination of $P_{\text{orb}} = 86.2$ min.

For the time being, we follow the usual convention and assume that high-velocity wings of the double-peaked emission lines originate in the inner accretion disc, and track the orbital motion of the white dwarf. A sine fit of the form $\gamma_1 - K_1 \sin[2\pi(t - T_{(1)0})/P_{\text{orb}}]$ to the H α radial velocity curve shown in Fig. 9 gives $T_{(1)0} = 2452932.3557 \pm 0.0003$ (HJD), $K_1 = 50 \pm 2 \text{ km s}^{-1}$ and $\gamma_1 = 8 \pm 1 \text{ km s}^{-1}$, with the orbital period fixed to 86.2 min. The amplitude K_1 is quite typical for the radial velocity variation of the emission line wings observed in short-period CVs (e.g. Thorstensen & Fenton 2003). The lack of eclipses in HS 2219+1824 does not allow us to establish absolute orbital phases. However, under the assumption that the wings of the emission lines come from disc material orbiting close to the white dwarf, the red-to-blue crossing of the radial velocities provides a rough estimate of the instant of inferior conjunction of the donor star (i.e. zero phase).

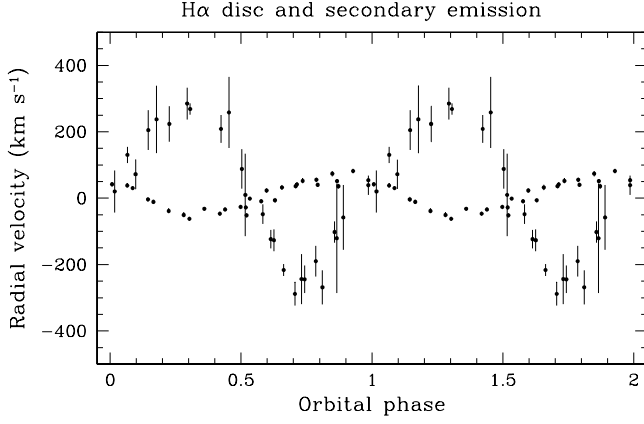


Fig. 10. $H\alpha$ radial velocity curves of the line wings and the chromospheric emission from the companion. The velocities are folded on the orbital period using $T_0 = 2452932.3485$ (HJD) and no phase binning has been applied. The orbital cycle has been plotted twice for continuity.

4.4. Detection of chromospheric emission from the companion star

The triple-peaked shape of the $H\alpha$ profiles (Fig. 7) suggests the presence of an additional narrow emission line component. This feature is intense enough to follow its motion by eye through almost all the individual profiles. We measured the velocities of this component by fitting single Gaussians after masking the rest of the line. The resulting radial velocity curve is presented in Fig. 9 (plotted as open triangles).

A sine fit to the velocities of the narrow component with the orbital period fixed provided $\gamma_2 = 28 \pm 7$ km s $^{-1}$ and $K_2 = 257 \pm 10$ km s $^{-1}$, but this time the curve is delayed by $\simeq 0.4$ orbital cycle with respect to the assumed zero phase. If the phasing of the radial velocity curve obtained from the $H\alpha$ wings indeed reflects the primary's motion, then the narrow emission originates at a location offset by $\simeq 140^\circ$ in azimuth from the white dwarf. A very likely source for a narrow emission line is the secondary star. The velocity amplitude of the narrow component is much larger than that of the broad line wings, in fact, $K_2 = 257$ km s $^{-1}$ is not unexpected for the orbital motion of the low-mass companion in a short period CV. We thus identify this narrow emission component as chromospheric emission from the donor star, possibly due to irradiation from the white dwarf/inner disc. Whereas narrow emission from the secondary star has been identified in short period dwarf novae during outburst (e.g. Steeghs et al. 2001), HS 2219+1824 is the first SU UMa dwarf nova where line emission from the secondary star is unambiguously detected in quiescence².

² Shafter et al. (1984) suggested the detection of the heated secondary during quiescence in IR Com ($P_{\text{orb}} = 98.5$ min) on the basis of a perturbation in the radial velocity curves of the emission lines. Secondary emission was also invoked in the eclipsing dwarf nova V893 Sco ($P_{\text{orb}} = 109.4$ min; Matsumoto

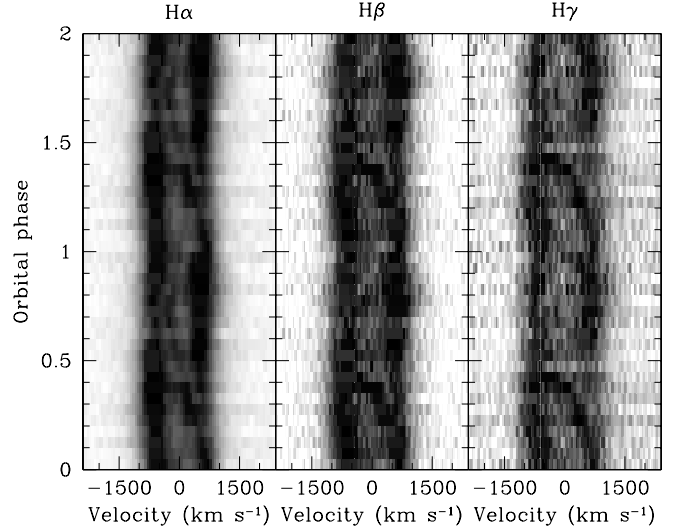


Fig. 11. $H\alpha$, $H\beta$ and $H\gamma$ trailed spectra diagrams. The spectra have been folded on the orbital period and averaged into 20 phase bins. Notice the narrow $H\alpha$ emission component from the secondary star. Another emission component with maximum blue velocity at $\varphi \sim 0.6-0.7$ is evident in $H\beta$. Dark represents emission and a full cycle has been repeated for continuity.

We will adopt the new $T_{(2)0} = 2452932.3485 \pm 0.0003$ (HJD) as the time of inferior conjunction of the secondary. The radial velocity curves of the disc and secondary emissions folded on the orbital period are shown in Fig. 10. The phase offset between both velocity curves is not exactly 0.5 cycle, which is not surprising as neither the velocity curves are perfectly sinusoidal nor are the emissions expected to come from the centres of the stellar components of the binary. Similar phase shifts have been observed in other systems before (e.g. Stover et al. 1981).

4.5. Trained spectrograms and Doppler tomograms

We have constructed trailed spectrograms of the $H\alpha$, $H\beta$ and $H\gamma$ lines from the continuum-normalised data. In order to enhance the signal-to-noise ratio we averaged the spectra into 20 orbital phase bins. The diagrams are presented in Fig. 11. All the lines clearly show the alternating changes in intensity of the double-peaked profiles. This is especially obvious in $H\alpha$, which also reveals the narrow emission component from the irradiated secondary with maximum excursion to the blue at $\varphi \sim 0.75$. Another emission S-wave is visible in $H\beta$ moving in between the double peaks. This component has the expected phasing for line emission from the bright spot region, with maxi-

et al. 2000) based on its $H\alpha$ Doppler tomogram, but V893 Sco has never undergone a superoutburst. The most reliable detection seems to have been made in the long-period SU UMa star TU Men ($P_{\text{orb}} = 168.8$ min), whose $H\alpha$ trailed spectra seem to show a narrow emission moving with the phasing of the secondary (Tappert et al. 2003), but its velocity semi-amplitude is almost the same as the double peak semi-separation so one must be cautious when interpreting their results.

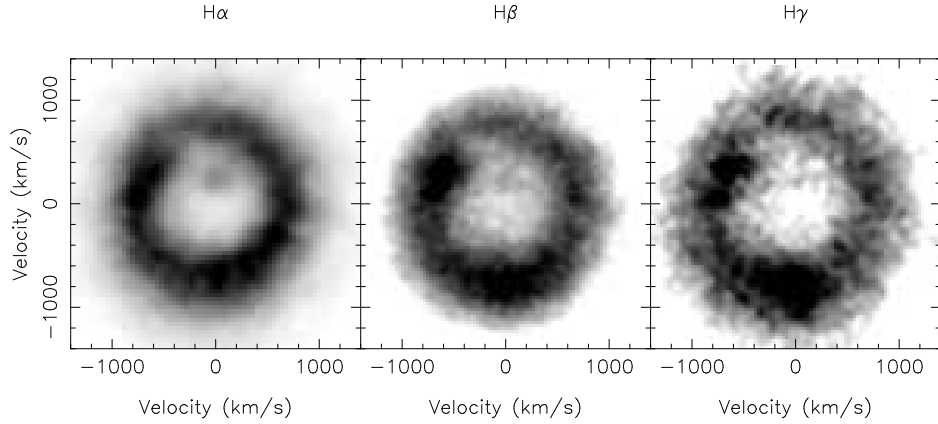


Fig. 12. H α , H β and H γ Doppler tomograms. Dark represents emission. Notice the H α emission at the location of the secondary and the two emission spots in H β and H γ .

mum blue velocity at $\varphi \sim 0.6-0.7$, and is strongest during the first half of the orbital cycle.

In order to map the line emission distribution in velocity space we computed Doppler maps of H α , H β and H γ using the maximum entropy technique developed by Marsh & Horne (1988). The tomograms are shown in Fig. 12. All the maps show a ring of emission, revealing the presence of an accretion disc. There is an emission spot in the H α map located at $(V_x \sim 0, V_y \sim +200)$ km s $^{-1}$, where emission from the secondary star is expected to be located in velocity space. This strongly supports our hypothesis of an origin of the narrow component seen in H α on the donor star in HS 2219+1824. Another emission spot is clearly seen in H β and H γ , superimposed on the disc emission at $(V_x \sim -450, V_y \sim +200)$ km s $^{-1}$. It is located close to the expected position of the bright spot, as its phasing in the trailed spectra already suggested. A third spot at $(V_x \sim 0, V_y \sim -600)$ km s $^{-1}$ can be seen in the H β and H γ tomograms, but the corresponding S-wave is not evident in the trailed spectra diagrams.

5. System parameters

5.1. The mass ratio

An estimate of the mass ratio $q = M_2/M_1$ of a CV can be obtained from its superhump fractional period excess, $\varepsilon = (P_{\text{sh}} - P_{\text{orb}})/P_{\text{orb}}$, through the relation (Patterson 1998):

$$\varepsilon = \frac{0.23 q}{1 + 0.27 q}. \quad (1)$$

In Sect. 3.2 we derived $\varepsilon = 0.032$, corresponding to a mass ratio of $q = 0.14$. The uncertainty in q is typically dominated by the scatter in the observed $q(\varepsilon)$ relation (and hence Patterson's 1998 fit to this relation) rather than by the uncertainty in ε .

We have measured in Sect. 4.3 and 4.4 the amplitudes of the radial velocity variations of the broad wings of the Balmer lines and of the narrow emission line component detected in H α . Attributing these radial velocity variations to material close to the white dwarf and on the

(irradiated face of the) secondary star, respectively, implies $K_1 \simeq 50$ km s $^{-1}$ for the radial velocity amplitude of the white dwarf and $K_2 \simeq 260$ km s $^{-1}$ for the secondary, which gives a mass ratio of $q = K_1/K_2 \simeq 0.19$, somewhat larger than the estimate from the fractional superhump period excess. If, as we suggest, the chromospheric emission of the secondary star originates primarily on the hemisphere facing the white dwarf then our K_2 underestimates the true radial velocity amplitude of the secondary, and this dynamical measure of q is an upper limit. We conclude that our observations suggest $0.14 \lesssim q \lesssim 0.19$.

5.2. The size of the accretion disc

We can also derive an estimate of the accretion disc radius from the measured double peak velocity separation. We have measured the semi-separation in the H α profiles which are not contaminated by the maximum velocity excursions of the S-waves, obtaining an average value of $V_d \approx 660$ km s $^{-1}$. This value gives a good estimate of the projected velocity of the outer disc edge. Smak (1981) provided a relation between the Keplerian projected velocity of the outer disc material, $V_K(R_d) \sin i$, where i is the orbital inclination of the system, and the velocity semi-separation of the peaks, V_d :

$$V_K(R_d) \sin i \simeq 0.95 V_d. \quad (2)$$

Combining this expression with Kepler's Third Law, and using $q = 0.14$, $M_1 \sim 0.7 M_\odot$, and $K_1 \lesssim 50$ km s $^{-1}$, we find $R_d \lesssim 0.54 R_{L1}$, where R_{L1} is the distance from the white dwarf to the inner Lagrangian point, given by Silber (1992). Thus the accretion disc in HS 2219+1824 in quiescence is probably quite small. The circularisation radius of the system is given by:

$$R_{\text{circ}} \approx \left(\frac{R_{L1}}{a} \right)^4 (1 + q), \quad (3)$$

where a is the binary separation. For HS 2219+1824, $R_{\text{circ}} \approx 0.38 R_{L1}$, smaller than the derived disc radius.

6. Conclusions

Based on our optical photometry and spectroscopy, we have identified HS 2219+1824 to be an SU UMa-type dwarf nova with an orbital period of $\simeq 86.2$ min and a superhump period of $\simeq 89.05$ min. The superoutburst amplitude is ~ 5.5 magnitudes, reaching $V \simeq 12$ at maximum. No normal outburst has been recorded so far. The broad $H\beta$, $H\gamma$, and $H\delta$ absorption lines observed in the optical spectrum of HS2219+1824 are consistent with the photospheric spectrum of a $13\,000\,\text{K} \lesssim T_{\text{eff}} \lesssim 17\,000\,\text{K}$ white dwarf at a distance of $180\,\text{pc} \lesssim d \lesssim 230\,\text{pc}$. The red part of the optical spectrum constrains the spectral type of the donor to be later than M5. Quiescent phase-resolved spectroscopy reveals an unusual narrow $H\alpha$ emission line component which we tentatively attribute to chromospheric emission from the irradiated inner hemisphere of the secondary star. The superhump fractional period excess and the radial velocities measured from this narrow $H\alpha$ component, as well as from the broad wings of the double-peaked emission lines suggest a mass ratio of $0.14 \lesssim q \lesssim 0.19$.

Acknowledgements. PRG and BTG were supported by a PPARC PDRA and a PPARC Advanced Fellowship, respectively. The HQS was supported by the Deutsche Forschungsgemeinschaft through grants Re353/11 and Re353/22. We are very grateful to Klaus Beuermann for giving us access to his M-dwarf spectral templates, and to Patrick Schmeer for alerting us of the 2004 outburst, as well as for drawing our attention to the ASAS-3 program.

References

- Abbott, T. M. C., Fleming, T. A., & Pasquini, L. 1997, *A&A*, 318, 134
- Araujo-Betancor, S., Gänsicke, B. T., Hagen, H.-J., Rodríguez-Gil, P., & Engels, D. 2003, *A&A*, 406, 213
- Araujo-Betancor, S., Gänsicke, B. T., Hagen, H.-J., et al. 2004, *IAU Coll 194 in press (astro-ph/0402270)*
- Bertin, E. & Arnouts, S. 1996, *A&AS*, 117, 393
- Beuermann, K., Baraffe, I., Kolb, U., & Weichhold, M. 1998, *A&A*, 339, 518
- Duerbeck, H. W. & Seitter, W. C. 1987, *Ap&SS*, 131, 467
- Gänsicke, B. T., Araujo-Betancor, S., Hagen, H.-J., et al. 2004, *A&A*, 418, 265
- Gänsicke, B. T., Beuermann, K., & de Martino, D. 1995, *A&A*, 303, 127
- Gänsicke, B. T., Beuermann, K., & Thomas, H. C. 1997, *MNRAS*, 289, 388
- Gänsicke, B. T., Fried, R. E., Hagen, H.-J., et al. 2000, *A&A*, 356, L79
- Gänsicke, B. T., Hagen, H. J., & Engels, D. 2002, in *The Physics of Cataclysmic Variables and Related Objects*, ed. B. T. Gänsicke, K. Beuermann, & K. Reinsch (ASP Conf. Ser. 261), 190–199
- Gänsicke, B. T., Sion, E. M., Beuermann, K., et al. 1999, *A&A*, 347, 178
- Gänsicke, B. T., Szkody, P., Howell, S. B., & Sion, E. M. 2004, *ApJ*, submitted
- Gilliland, R. L., Kemper, E., & Suntzeff, N. 1986, *ApJ*, 301, 252
- Greenstein, J. L. 1957, *ApJ*, 126, 23
- Hamada, T. & Salpeter, E. E. 1961, *ApJ*, 134, 683
- Horne, K. 1986, *PASP*, 98, 609
- Marsh, T. R. & Horne, K. 1988, *MNRAS*, 235, 269
- Matsumoto, K., Mennickent, R. E., & Kato, T. 2000, *A&A*, 363, 1029
- Mennickent, R. 1994, *A&A*, 285, 979
- Mukai, K., Mason, K. O., Howell, S. B., et al. 1990, *MNRAS*, 245, 385
- Nogami, D., Engels, D., Gänsicke, B. T., et al. 2000, *A&A*, 364, 701
- Patterson, J. 1998, *PASP*, 110, 1132
- Patterson, J., Thorstensen, J. R., Kemp, J., et al. 2003, *PASP*, 115, 1308
- Pojmański, G. 2001, in *ASP Conf. Ser. 246: IAU Colloq. 183: Small Telescope Astronomy on Global Scales*, 53
- Rodríguez-Gil, P., Gänsicke, B. T., Araujo-Betancor, S., & Casares, J. 2004a, *MNRAS*, 349, 367
- Rodríguez-Gil, P., Gänsicke, B. T., Barwig, H., Hagen, H.-J., & Engels, D. 2004b, *A&A*, 424, 647
- Scargle, J. D. 1982, *ApJ*, 263, 835
- Schneider, D. P. & Young, P. 1980, *ApJ*, 238, 946
- Schwarzenberg-Czerny, A. 1989, *MNRAS*, 241, 153
- Shafter, A. W. 1983, *ApJ*, 267, 222
- Shafter, A. W., Cowley, A. P., & Szkody, P. 1984, *ApJ*, 282, 236
- Shafter, A. W., Veal, J. M., & Robinson, E. L. 1995, *ApJ*, 440, 853
- Silber, A. D. 1992, *Ph.D. Thesis*
- Sion, E. M., Leckenby, H. J., & Szkody, P. 1990, *ApJ Lett.*, 364, L41
- Smak, J. 1981, *Acta Astronomica*, 31, 395
- Steeghs, D., O'Brien, K., Horne, K., Gomer, R., & Oke, J. B. 2001, *MNRAS*, 323, 484
- Stover, R. J., Robinson, E. L., & Nather, R. E. 1981, *ApJ*, 248, 696
- Szkody, P., Gänsicke, B. T., Sion, E. M., & Howell, S. B. 2002, *ApJ*, 574, 950
- Szkody, P., Gänsicke, B., Fried, R. E., Heber, U., & Erb, D. K. 2001, *PASP*, 113, 1215
- Tappert, C., Mennickent, R. E., Arenas, J., Matsumoto, K., & Hanuschik, R. W. 2003, *A&A*, 408, 651
- Thorstensen, J. R. & Fenton, W. H. 2003, *PASP*, 115, 37
- Williams, R. E. 1980, *ApJ*, 235, 939